Rev. Mexicana Astron. Astrof., **25**, 51-57 (1993)

CALAN-TOLOLO SURVEY. V: TWO HUNDRED NEW SOUTHERN QUASARS

José Maza[1], María Teresa Ruiz[1], Luis E. González[1]
Marina Wischnjewsky[1], and Roberto Antezana

Departamento de Astronomía
Universidad de Chile

Received 1992 November 3

RESUMEN

Se presenta la quinta lista de la Exploración Calán-Tololo. Contiene información acerca de 200 cuasares australes no conocidos anteriormente. La mayoría de los objetos tienen una magnitud B en el intervalo $17 \leq B < 19$ con 14 cuasares más brillantes que 17 y 24 más débiles que 19. Los corrimientos al rojo de los cuasares son tales que, la mayor parte cumplen con la desigualdad: $1.8 \leq z \leq 3.4$; sólo 36 objetos tienen un corrimiento al rojo menor que 1.8. El cuasar típico tiene $B \sim 18.3$ y $z \sim 2.1$. Estos cuasares fueron encontrados en Cerro Calán explorando placas de prisma objetivo tomadas en Cerro Tololo usando la cámara Curtis-Schmidt con el prisma ultravioleta delgado y placas Eastman Kodak IIIa-J. Presentamos cartas de identificación, coordenadas ecuatoriales, una estimación de la magnitud azul, B, y un corrimiento al rojo preliminar. Todos los cuasares de esta lista han sido confirmados espectroscópicamente, utilizando el telescopio de 4 metros de Cerro Tololo o el telescopio du Pont de 2.5 metros del Observatorio de Las Campanas. Esta información será publicada posteriormente (Maza y Ruiz 1993).

ABSTRACT

The fifth list of the Calán-Tololo Survey is presented. It contains information for 200 new southern quasars. Most objects have a B magnitude in the range $17 \leq B < 19$; 14 objects are brighter than 17th and 24 fainter than 19th. The redshift z of most quasars satisfies the inequality: $1.8 \leq z \leq 3.4$; only 36 quasars have redshifts lower than 1.8. The typical quasar has $B \sim 18.3$ and $z \sim 2.1$. These quasars were found at Cerro Calán, searching objective prism plates taken at Cerro Tololo using the Curtis-Schmidt telescope, the thin *UV* prism and Eastman Kodak IIIa-J plates. We present identification charts, equatorial coordinates, an estimated blue magnitude and a preliminary redshift for every object. All quasars in this list have been confirmed using slit spectroscopy at the CTIO 4-m telescope or at the Las Campanas Observatory 2.5-m du Pont telescope. The spectroscopic data shall be presented elsewhere (Maza & Ruiz 1993).

Key words: **QUASARS**

1. INTRODUCTION

Quasi-stellar objects, quasars, remain as a major challenge to contemporary astrophysics after three decades of very significant efforts by a large number of astronomers all over the world. A great deal has been learned about quasars since the realization by Schmidt (1963) that 3C 273 is an object with an unusually high redshift ($z = 0.158$).

At the beginning quasars were found as radio sources; later on many were added to the list because they were characterized as having a large ultraviolet flux of radiation, an ultraviolet excess relative to a stellar flux distribution. This ultraviolet excess led to the color technique for discovering quasars [stellar objects with $(U-B) < -0.30$] that has been very successfully used to find quasars up to a redshift $z \sim 2.2$; at higher redshifts the usually strong Lyman alpha line (Lα) entering the B band makes the $U-B$ color redder than -0.30.

[1] Visiting Astronomer at Cerro Tololo Inter-American Observatory, National Optical Astronomy Observatories, operated by the Association of Universities for Research in Astronomy under contract with the National Science Foundation of the U.S.A.

Objective prism techniques have been used extensively in astrophysical inquiry since 1885 when E.C. Pickering started the Henry Draper Memorial Project, the beginning of modern spectral classification (see Hoffleit 1991). Soon after the discovery of quasars B.E. Markarian started a large objective prism survey to search for galaxies with a strong ultraviolet continuum and quasars that produced a strong impact on the number of Seyfert galaxies known. During the seventies M. Smith conducted the Tololo Survey (Smith 1975; Smith, Aguirre, & Zemelman 1976) and G. MacAlpine, the Michigan Survey (MacAlpine, Lewis, & Smith 1977; MacAlpine, Smith, & Lewis 1977*a*, 1977*b*; MacAlpine & Lewis 1978; MacAlpine & Williams 1981). These surveys were very successful discovering high redshift quasars.

During 1985 we started an extension of the Tololo Survey in order to discover new bright quasars and Seyfert galaxies in the southern hemisphere, along with starburst galaxies, carbon stars, cataclysmic variable stars, etc. The Calán-Tololo Survey (herein after CTS) is an objective prism survey conducted at Cerro Calán (Department of Astronomy, University of Chile), using the Curtis-Schmidt telescope at Cerro Tololo Inter-American Observatory (CTIO). The main goal of the CTS is the discovery of new emission line galaxies and quasars in a large area of the southern sky. A description of the survey, the procedure and other details can be found in Maza et al. 1988*a*, 1988*b*, 1989, 1991 and 1992.

List No. 1 of the Calán-Tololo Survey containing 30 new Seyfert 1 galaxies was published in 1989 (Maza et al. 1989). List No. 2 presenting 40 Seyfert 1 galaxies is in Maza et al. 1992. List No. 3 containing 42 H II galaxies was published in 1991 (Maza et al. 1991). List No. 4 presenting 40 Seyfert 1 galaxies is in preparation (Maza et al. 1993). The present list contains information for 200 new quasars discovered in the Calán-Tololo Survey and fully confirmed during the spectroscopic follow-up at CTIO and at Las Campanas Observatory.

2. OBSERVATIONS

Photographic plates have been obtained for 163 fields in the southern hemisphere at galactic latitude b such that $|b| \geq 20°$, covering 3400 deg^2 (see Figure 1 in Maza et al. 1989). We have used the Curtis-Schmidt telescope equipped with the thin *UV* prism that yields a reciprocal dispersion of 1740 A/mm at Hβ, 1340 A/mm at Hγ, and 1100 A/mm at λ 3727 A (Blanco 1974). We have used Eastman Kodak IIIa-J plates baked in forming gas and exposed to the sky limit (90 minutes) without trailing. Objects as faint as 19th magnitude are visible at the plate limit. The spectral resolution at the plate scale of the Curtis-Schmidt (97″/r is ~30 A for a seeing of 2″. The strong emis lines present in the spectrum of a high red: quasar (Lα most of the time) are resolved on objective prism plates. This makes confusion high redshift starburst galaxies very small. method of selecting a quasar candidate relies ma on the presence of emission lines. The most f rable situation to select a quasar candidate on objective prism plates is that when Lα is near 4 A and the C IV (1549 A) is near 5000 A; corresponds to a redshift z = 2.2 (see Figure Pesch 1991, for sketches of the spectra of qua on this type of plates). The lines that allow candidates to be selected on the objective-p plates are: the blend Lα + N V at 1240 A in r cases (82%), C IV at 1549 A and Mg II at 2798 roughly 8% each, and C III] at 1909 A in very cases ($\leq$ 2%). A small number of broad absorp line quasars (BAL's) have been found because t spectra look quite conspicuous on the plates, sin to the spectra of unusual carbon stars (see § 4).

Quasar candidates have been confirmed as sars using slit spectroscopy at CTIO; the 4-m escope and to a lesser extent the 1.5-m teles with cassegrain spectrographs have been used this purpose over the last five years. Many cand tes have also been confirmed as quasars using 2.5-m du Pont telescope at Las Campanas servatory (Carnegie Southern Observatory in le). The details of the spectrophotometry sha reported elsewhere (Maza & Ruiz 1993).

3. LIST No. 5

Figure 1 (Plate) presents identification ch and Table 1 the corresponding data for the 200 new quasars found and confirmed so fa the CTS. Equatorial coordinates were obta measuring the objective-prism plates, using ASCORECORD Carl Zeiss Jena X-Y engin Cerro Calán. Reference stars used are from Perth-70 Catalog (Høg et al. 1976). The spe are always oriented north-south on the plates, wavelength increasing to the south. As the hea each spectrum was measured (the long wavele end at 5350 A) a significant error in declinatic inevitable for faint objects; these quasars are s 10 magnitudes fainter than the reference s We know from previous experience with ca stars in the Magellanic Clouds (of B magnit comparable to the present group of quasars) these types of coordinates are 13 ± 7 arcsec displaced to the north. That shift depends on the apparent magnitude of the object and the sl of the continuum near 5350 A. Given the va of spectral distributions and magnitudes for t quasars no correction to the measured coordir

TABLE 1

CALAN-TOLOLO SURVEY LIST No. 5: QUASARS

Object	α (1950)	δ	B	z
16.06	$0^h\ 5^m\ 43.1^s$	−46° 27′ 43″	17.9	1.88
16.07	0 6 6.0	−46 36 13	17.8	1.85
17.05	0 12 3.2	−46 47 34	18.2	2.22
19.02	0 54 54.6	−47 3 48	18.9	2.0:
16.09	1 0 47.3	−42 20 3	17.7	2.33
20.06	1 28 40.1	−43 36 42	18.7	2.50
21.03	1 47 6.4	−33 39 32	17.2	1.7
19.01	1 50 29.9	−38 59 39	19.2	2.0:
19.06	1 51 0.1	−40 31 32	18.1	2.8:
19.09	1 57 24.5	−40 57 33	18.2	2.02
22.30	2 2 9.9	−46 2 5	18.3	1.88
22.31	2 2 37.4	−46 13 31	19.1	3.24
19.14	2 3 35.6	−39 41 42	18.0	2.60
19.16	2 6 1.1	−39 30 35	18.2	2.2
20.10	2 13 5.5	−38 37 55	18.1	1.63
20.11	2 14 19.5	−39 21 35	18.0	2.75
24.01	2 25 5.2	−44 57 19	19.2	1.70:BAL
20.15	2 27 17.5	−40 23 56	19.3	1.75:BAL
24.09	2 35 47.9	−45 29 24	17.9	1.70:BAL
23.16	2 39 20.9	−36 45 41	19.2	3.10
21.07	2 46 56.3	−40 46 31	16.3	1.74
24.03	2 50 56.5	−46 42 42	18.3	1.88:BAL
25.34	2 53 33.7	−46 35 45	18.2	2.06
25.35	2 55 32.0	−46 52 36	18.7	1.85
25.36	3 0 7.2	−43 42 25	19.2	2.3:
25.27	3 0 41.2	−42 50 33	17.7	2.0
25.28	3 1 2.1	−42 45 40	19.1	1.93
25.29	3 2 20.4	−45 15 16	17.3	1.0
25.02	3 6 58.0	−35 1 48	18.0	1.4
25.03	3 8 6.1	−37 34 40	17.7	0.40
26.05	3 10 53.0	−43 50 11	19.2	2.66
25.07	3 14 19.7	−37 15 38	18.1	1.12
26.07	3 15 13.2	−46 20 21	18.3	2.45
25.12	3 16 17.7	−45 9 39	17.9	1.66
26.09	3 20 14.3	−44 38 35	18.7	2.08
26.09	3 26 45.0	−34 30 23	17.9	1.35
26.31	3 28 10.4	−46 16 40	19.2	2.08
26.13	3 28 32.2	−46 36 8	19.3	3.10
26.14	3 31 3.7	−45 5 44	17.9	2.6
27.07	3 35 24.0	−43 10 1	18.1	2.58
25.09	3 42 10.0	−38 42 5	18.7	2.45
28.03	3 45 25.8	−44 34 55	17.9	2.47
28.05	3 47 28.4	−45 3 29	18.8	2.90
28.13	3 48 6.9	−45 5 53	18.2	2.12
28.16	3 57 59.4	−43 13 40	17.7	1.51
27.05	4 2 6.9	−33 42 54	18.0	3.04
29.01	4 5 41.8	−44 17 58	17.6	3.00
29.08	4 7 27.8	−45 19 43	17.5	1.84
28.09	4 9 37.0	−34 1 3	17.5	1.35
28.07	4 10 6.7	−43 2 12	16.7	2.40
26.05	4 13 7.4	−38 16 29	18.8	2.4:
29.10	4 16 38.1	−45 39 26	17.5	2.5
29.03	4 19 20.2	−45 30 57	17.9	2.45

N	Object	α (1950)	δ	B	z
254	A29.06	4 28 26.6	−36 32 59	18.0	2.09
255	F27.14	4 35 32.6	−30 41 19	17.9	2.1:
256	A29.20	4 41 28.0	−36 51 45	17.2	0.68
257	F27.26	4 42 18.0	−30 9 58	18.1	2.40
258	A29.22	4 43 46.5	−35 52 7	18.3	2.61
259	B27.07	4 43 53.6	−40 53 59	18.9	3.27
260	F27.21	4 43 57.9	−32 3 51	17.8	3.00
261	B27.06	4 45 21.8	−41 51 4	17.8	2.70
262	C30.10	4 45 51.0	−45 42 37	17.2	0.91
263	F27.24	4 45 51.7	−30 47 2	18.0	2.42
264	A30.15	4 51 11.2	−33 38 43	17.33	1.8
265	A30.19	4 54 53.3	−34 25 52	18.1	2.43
266	A30.25	4 59 25.9	−37 18 31	18.5	1.93
267	A30.13	5 0 3.8	−33 33 36	17.0	2.0
268	A30.20	5 1 54.9	−34 4 11	18.0	2.8
269	A31.05	5 15 59.5	−37 57 33	18.3	3.02
270	A31.07	5 18 11.5	−35 0 43	18.2	2.23
271	B30.05	5 32 58.9	−42 25 55	18.0	2.81
272	A32.02	5 46 16.5	−35 43 8	17.7	2.45
273	B31.05	5 50 33.4	−38 28 57	18.0	2.13
274	A33.03	5 56 28.8	−36 19 50	18.1	2.22
275	B31.18	6 2 47.3	−39 50 58	18.2	2.2
276	A34.09	6 8 1.2	−35 14 55	17.2	0.81
277	M98.06	9 27 44.5	−25 47 5	17.9	2.15
278	R02.37	9 31 19.8	−16 55 43	17.8:	0.32
279	J01.09	9 35 12.8	−19 58 48	18.9	2.21
280	J01.03	9 37 30.2	−18 18 20	16.2	2.4:
281	M00.21	9 50 15.5	−23 39 36	18.64	3.0:
282	M00.04	9 52 58.6	−25 3 5	17.8	2.4:
283	M00.08	9 53 5.3	−23 18 8	18.92	2.0:
284	J02.11	9 56 47.5	−20 43 22	18.00	1.90
285	J02.03	10 7 27.8	−17 25 34	18.08	2.60
286	J03.13	10 15 1.0	−20 31 44	17.08	2.80
287	J03.14	10 15 59.3	−21 24 53	17.95	2.47
288	J03.16	10 23 31.6	−21 25 0	18.69	2.5
289	M02.28	10 25 49.1	−26 28 44	17.87	2.9:
290	J03.23	10 27 23.8	−19 48 25	19.2	2.12
291	M02.18	10 31 37.8	−24 58 41	17.2	2.9:
292	M02.34	10 37 41.8	−26 37 56	18.1	2.0:
293	R05.12	10 41 27.2	−14 47 30	18.4:	2.12
294	R05.17	10 43 8.4	−15 12 46	19.2:	2.12
295	J05.03	10 54 59.0	−20 44 32	17.9	2.10
296	M05.11 M	10 55 44.3	−25 49 35	17.79	3.0:
297	J06.07	11 10 29.4	−18 24 7	19.3	2.96
298	R07.04	11 11 21.1	−15 17 24	18.7:	3.37
299	R07.27	11 22 12.3	−16 48 41	17.7:	2.95
300	R07.16	11 25 47.0	−13 2 50	16.61	0.43
301	K03.02	11 28 49.6	−28 50 19	17.6	2.30
302	R08.06	11 37 53.9	−12 43 48	17.2:	2.29
303	J07.05 S	11 40 19.6	−21 30 4	16.9	0.39
304	J07.06 S	11 46 45.2	−19 11 1	19.2	2.00
305	R09.66	11 50 9.4	−16 16 4	18.7:	2.50
306	J08.06 S	11 57 7.4	−19 42 42	16.2	0.45

TABLE 1 (CONTINUED)

N	Object	α (1950)	δ (1950)	B	z	
307	M08.02	11 57 28.8	−23 54 30	17.67	2.1::	BAL
308	R09.11	11 59 24.9	−13 38 4	17.2:	0.50	
309	R10.07	12 11 11.7	−13 22 0	16.14	0.43	
310	R10.29	12 20 36.8	−15 27 20	18.7:	0.44	
311	R10.30	12 23 22.2	−15 43 37	16.2:	1.74	
312	R10.25	12 25 51.4	−13 47 21	19.2:	2.26	
313	M10.08 M	12 30 27.6	−23 47 2	16.73	1.80	
314	K06.08	12 33 6.1	−30 34 16	18.7	3.1	
315	R11.12	12 33 42.4	−14 10 36	17.7:	0.8	
316	R12.24	12 57 46.7	−16 32 9	17.2:	2.22	
317	M12.31	12 57 54.3	−24 15 32	18.39	2.0:	
318	M12.24	12 59 7.6	−22 36 19	18.54	2.00	
319	M12.30	13 6 16.7	−25 8 48	18.7	2.1	
320	K08.03	13 14 57.0	−31 31 9	18.2	3.10	
321	R13.07 M	13 15 5.5	−14 1 9	16.7:	0.43	
322	K08.01	13 22 30.8	−29 34 53	17.64	2.44	
323	R14.09 M	13 35 33.4	−14 21 25	18.7:	1.92	
324	J13.07	13 39 21.3	−18 2 45	17.34	2.21	BAL
325	R14.07 M	13 40 18.1	−13 40 55	19.2:	3.19	
326	M14.25	13 42 13.0	−24 45 56	19.2	2.8	
327	M15.16	13 52 56.3	−22 42 27	18.2	2.0:	
328	R15.04	13 54 0.4	−13 34 35	18.2	2.1:	
329	M15.19	13 55 10.6	−24 37 15	17.9	1.37	
330	M15.17	13 56 32.2	−22 43 12	19.1	2.11	
331	R15.03	13 58 56.0	−13 31 21	18.7:	3.1	
332	R15.07	13 59 30.3	−15 30 31	17.54	2.45	
333	J15.32	14 13 53.9	−21 17 53	17.9	2.3	
334	R16.21	14 14 27.3	−17 9 35	17.7::	2.54	
335	M16.09	14 17 1.1	−25 4 29	18.0	1.88	
336	K11.04	14 20 34.2	−29 31 59	18.27	2.7:	
337	M16.07	14 24 7.5	−25 26 29	18.2	2.2:	
338	R16.06 M	14 25 2.9	−13 38 20	17.19	2.00	
339	M16.08	14 28 26.3	−23 50 31	17.3	1.88	
340	R17.08 M	14 31 41.8	−16 36 20	17.3:	2.45	
341	R18.18 M	14 55 10.6	−14 8 34	17.74	2.04	
342	M19.06	15 21 5.0	−24 36 7	17.8	2.10	
343	C05.07	20 9 49.1	−47 5 54	17.78	2.37	
344	A05.06	20 34 22.1	−33 11 3	17.2	1.90	
345	A05.05	20 34 37.4	−33 16 44	18.0	1.09	
346	A05.09	20 44 47.8	−37 1 0	18.7	2.10	
347	A06.17	21 3 40.4	−34 42 50	18.8	1.8	
348	A06.11	21 4 55.1	−36 18 24	18.0	2.04	
349	C07.35	21 8 38.7	−43 57 30	18.2	2.25	
350	C07.21	21 11 51.2	−43 35 19	17.6	1.70	
351	A07.01 S	21 12 1.7	−36 24 57	18.0	2.37	
352	C07.07	21 13 23.6	−43 5 12	17.5	0.1::	
353	C08.04	21 14 3.5	−43 46 36	18.2	2.00	
354	C08.03	21 14 10.8	−43 35 18	17.8	2.00	
355	B05.03	21 18 4.8	−41 24 13	17.8	1.80	
356	B05.02	21 18 14.9	−40 17 51	18.2	2.90	
357	A08.01	21 28 33.3	−35 32 2	18.4	3.19	
358	B06.02	21 38 40.4	−38 54 2	19.2	3.10	
359	B06.03	21 39 49.2	−42 1 34	19.3	2.40	
360	A09.40	21 46 26.7	−33 55 21	18.7	2.5	
361	A09.70	21 47 14.5	−37 15 28	18.3	2.7	
362	A09.22 S	21 48 25.9	−33 47 12	18.2	2.13	
363	A09.02 S	21 48 41.5	−36 16 22	18.3	2.29	
364	A09.44	21 54 56.5	−34 35 12	17.2	1.88	
365	A09.51	21 56 6.4	−34 52 16	19.2	2.21	
366	A09.60	21 56 56.2	−35 57 10	17.0	1.8	
367	A09.09 S	21 57 38.8	−35 16 45	17.2	2.70	
368	A09.31 S	21 58 26.0	−32 46 11	18.1	2.13	
369	A09.14 S	21 58 55.1	−33 59 5	18.0	2.21	
370	A09.24 S	21 59 19.6	−33 17 50	17.0	1.51	
371	A09.65	21 59 44.8	−36 24 42	18.0	2.01	
372	A09.15 S	22 1 10.6	−33 33 20	18.2	1.98	
373	A09.62	22 1 39.0	−36 7 30	18.4	1.54	
374	A09.23 S	22 2 40.2	−34 40 41	18.7	2.87	
375	A09.57	22 3 41.8	−35 41 0	19.5	3.25	
376	A09.85SS	22 8 33.7	−35 4 39	19.5	2.4	
377	A09.72	22 8 53.1	−37 21 42	16.1	0.32	
378	A09.36	22 8 54.7	−33 10 18	16.7	0.31	
379	A09.55	22 9 19.6	−34 59 30	17.5	1.94	
380	A09.20 S	22 10 4.0	−35 56 5	18.3	1.96	
381	A09.50	22 10 50.6	−34 15 35	17.9	2.4	
382	A10.11S	22 12 40.9	−33 28 24	18.7	2.28	
383	A10.20 S	22 13 34.7	−37 22 24	17.9	1.92	
384	A10.09 S	22 26 11.3	−33 30 26	16.4	0.86	
385	A11.31	22 31 2.9	−36 8 7	17.9	1.91	
386	C12.03	22 33 33.9	−46 59 19	17.8	2.3:	
387	A11.17 S	22 39 40.1	−36 59 59	18.4	2.8	
388	B09.08	22 43 53.7	−38 42 32	18.7	2.19	
389	B09.07	22 45 11.9	−37 59 20	17.6	2.02	
390	A11.35	22 46 38.5	−36 7 3	18.1	2.7	
391	A11.09	22 50 22.2	−37 13 54	18.2	3.2	
392	A11.45	22 50 56.7	−36 2 36	18.9	2.08	
393	A12.03	22 57 16.0	−34 29 10	19.2	2.20	
394	C14.27	23 10 6.9	−45 8 47	18.2	1.92	
395	A13.02	23 13 13.6	−33 55 59	18.3	2.9	
396	A13.04	23 14 0.8	−34 5 25	18.9	3.1	
397	A13.01	23 15 41.9	−33 51 35	18.3	2.07	
398	C15.41	23 36 38.8	−46 14 49	18.4	2.19	
399	C15.40	23 38 22.8	−46 22 2	18.2	2.64	
400	C16.04	23 55 34.4	−46 21 35	16.9	2.37	

was applied but the reader is warned that the true position on the sky for many quasars in Table 1 could be from 5 to 25 arcseconds to the south of the coordinates we have given. The accuracy of the R.A. coordinates is estimated to be ± 4 arcseconds.

Several steps were taken to reduce the impact of this type of error in the measuring process. We used a direct plate taken with the Maksutov astrograph at the Cerro El Roble Astronomical Station of the University of Chile if we had such a plate available.

e Maksutov telescope has a meniscus aperture 0.70-m and 2.1-m focal length (a plate scale of '/mm). The co-ordinates determined using these tes have errors of ±1″. In all cases where a po- on from a Maksutov plate was available those the figures given in Table 1, and indicated by etter M before the right ascension. For a few jects a direct Curtis-Schmidt plate was available l measured. The errors in this case for both co- linates are ±2″; those are indicated by a letter S Table 1.

B magnitudes were estimated from the ESO ick Blue Chart for most objects. The CCD se- ences F284-8 and F342-10 from Stobie, Sagar, & more (1985) were used to calibrate (guide) the estimates. For 26 quasars a CCD B magnitude been obtained by Maza & Takamiya (1993). mparing our eye estimated magnitudes with the CD magnitudes a systematic shift of −0.34 ± 0.29 s found. All magnitudes were then corrected −0.3 magnitudes; the values for B presented in ble 1 are the corrected magnitudes. The un- tainty of the quoted magnitudes is of the order 0.3 magnitudes. For 26 objects the CCD value m Maza & Takamiya (1993) is presented with 2 cimal places in Table 1. For a few objects, north declination −17.5° a Maksutov plate was used to imate the B magnitude; the uncertainty for those ues is greater (~ ± 0.7) and they are indicated by olon in Table 1.

The last column of Table 1 presents a prelim- ry redshift value. These figures were obtained ually at the telescope when the spectroscopic nfirmation of the quasar was made. Uncertain lues are indicated by a colon or by a double colon ien the line or lines present had not been fully entified. The details of the spectrophotometry all be presented elsewhere (Maza & Ruiz 1993). ie figures given here are just a general orientation r prospective observers. Six quasars present oad absorption lines; they are indicated as "BAL" er the redshift value.

4. STATISTICAL PROPERTIES

This sample of two hundred quasars is large ough to try to get some preliminary statistical operties of the objects found in the CTS but ing just the first list it is composed mainly of ry good candidates, those with very strong lines. hat follows supersedes a very preliminary redshift stribution given by Maza et al. 1988*b*.

A preliminary analysis of the redshifts found in ir survey is presented in Figure 2. The histo- am shows the CTS quasars have a very strong eference for redshifts such that 1.8 ≤ z < 3.4 (164 iasars out of 200, that is 82%) meaning that the end *Lα* + N V is the best feature to discover a

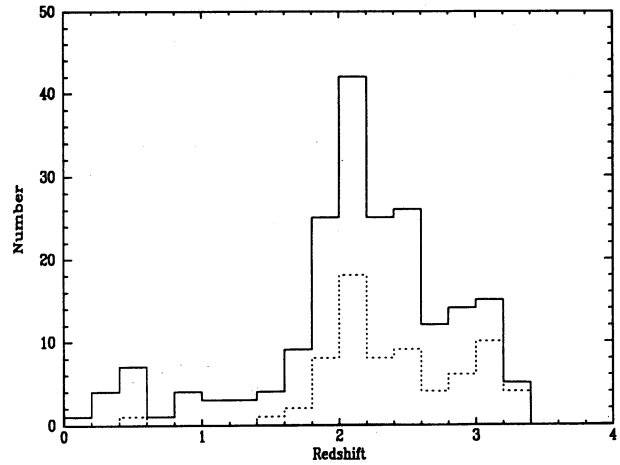

Fig. 2. Histogram of the redshift distribution of Calán-Tololo quasars. Solid line represents the total sample (200 objects); dashed line corresponds to the faint end of the sample (B > 18.25) involving 70 objects. A total of 118 quasars (59%) have a redshift z such that 1.8 ≤ z < 2.6; 173 quasars (86.5%) have z such that 1.6 ≤ z < 3.4.

quasar in our survey. A few objects were selected because the Mg II line (2798 A) was visible on the objective prism spectrum; those objects have 0.2 ≤ z < 1.0; Figure 2 shows 16 objects (8%) discovered by the Mg II line. In the upper edge of that redshift interval 0.8 ≤ z < 1.0 the small enhancement seen in Figure 2 (four quasars) might be due to the fact that the C III] line at 1909 A also guided the discovery. We can conclude the Mg II oriented less than 8% and C III], 2% of our candidates. For a group of quasars the C IV line (1549 A) was the key line to pick up that candidate (19 objects have 1.0 ≤ z < 1.8). The number of quasars found for the redshift interval 1.6 ≤ z < 1.8 increased from an average of 3 to 4 in the previous intervals to 9. This probably means that the blend Lα + N V is also helping to discover a fraction of those quasars (Lα is located in the wavelength range 3160 A to 3400 A if 1.6 ≤ z < 1.8). Therefore the percentage of quasars found by the C IV 1549 A line is less than 9%, probably around 7%. Our survey is not effective at discovering low redshift quasars (0.2 ≤ z < 1.8) because we have not selected quasar candidates just because the continuum color is too blue. For very low redshifts (z < 0.3) we have found more than one hundred so far, but we call those Seyfert 1 galaxies (see Maza et al. 1989, 1992, 1993).

Figure 3 shows the histogram of the B magnitudes of Table 1. Fourteen objects have B < 17 and twenty four objects have B > 19. Therefore 162 objects out of 200 (81%) have 17 ≤ B < 19. A large

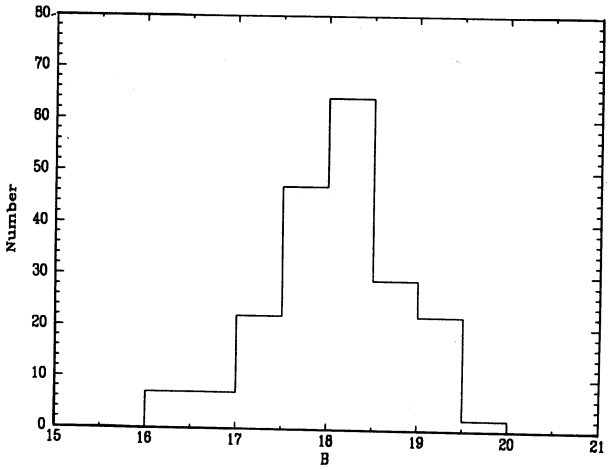

Fig. 3. Histogram of the B magnitude distribution of the Calán-Tololo quasars. One hundred and twelve objects (56%) have B such that $17.5 \leq B < 18.5$. Fourteen objects have $B < 17$; twenty four have $B \geq 19$. A total of 162 quasars (81%) have B such that $17 \leq B < 19$.

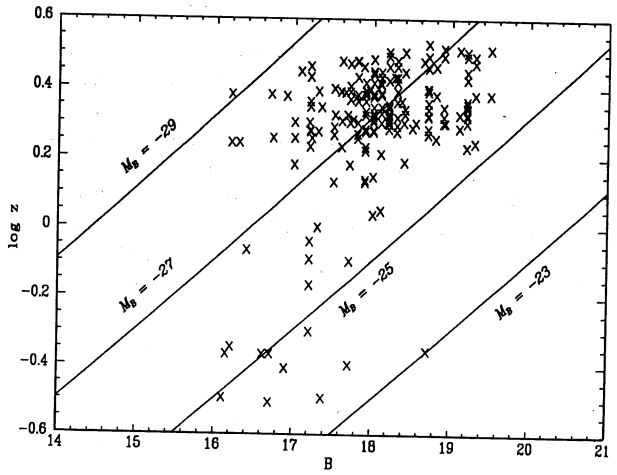

Fig. 4. Hubble diagram for Calán-Tololo quasars. 90% of the objects have M_B in the range -25 to -29. Lines of absolute magnitudes were computed for $H_0 = 60$ km s^{-1} Mpc^{-1}, $q_0 = 0.5$ and $\alpha = -0.5$.

peak is seen in the interval $18 \leq B < 18.5$ with 64 objects (32% of the sample). Figure 3 suggests the CTS is effective up to $B \sim 18.5$ where it becomes severely incomplete.

The probability of discovery for a quasar on objective prism plates depends – among other factors – on the equivalent width of the emission line present in the spectrum. For quasars with B between 18.0 and 18.5 the probability of detection on the Curtis-Schmidt plate is a very steep function of the equivalent width in the range from 150 A to 500 A (see Figure 1 in Gratton & Osmer 1987). As the blend Lα + N V is always 2.5 to 3 times stronger than C IV the numbers found here (a ratio 10:1 for quasars discovered by Lα + N V to those by C IV) are in a general good agreement with the model suggested by Gratton & Osmer for the probability of these discoveries.

The quasars found by the Mg II line are on the average brighter than those detected by C IV and so in spite of the fact that usually C IV is 2.5 times stronger than Mg II they are found in roughly the same proportion (the probability of detection rises quickly with apparent magnitude; see again Figure 1 in Gratton & Osmer 1987).

Figure 4 presents a Hubble diagram for these Calán-Tololo quasars. Lower redshift quasars tend to be brighter. Diagonal lines present the locus for $M_B = -23, -25, -27$, and -29, for $H_0 = 60$ km s^{-1} Mpc^{-1}, $q_0 = 0.5$ and $\alpha = -0.5$ (Weedman 1986). Low redshift quasars in the CT sample have M_B in the range -23 to -25 whereas high redshift objects have on average $M_B = -27$. Objects with $z < 1.8$ ($\log z < 0.26$) are few (36) and those with $z < 0.6$ ($\log z < -0.22$) are sparse (12). No statistical properties can be drawn for them.

Figure 4 also shows what might be an additional bias in the sample: quasars with $B > 18.25$ are either high redshift quasars ($z \sim 3.1$; [Lα + N V] $\sim$ 5200 A) or they have a redshift $z \sim 2.1$ [Lα + N V] $\sim$ 3800 A). For objects in the magnitude range $17.5 \leq B \leq 18.25$ the blend [Lα + N V] can be anywhere from 3500 A to 5300 A and the quasar has a good probability to be selected. For fainter objects (those with $B > 18.25$) it seems that if [Lα + N V] is located from 3900 A to 4900 A the probability of discovery diminishes more rapidly. Figure 2 shows as a dashed line the histogram that corresponds to objects fainter than 18.25. Better B magnitudes are necessary to assess the reality of this effect. If real it could be due to a complex combination of a selection bias produced by the photographic emulsion plus the telescope optics sensitivity, a subjective selection criterion and the fact that higher redshift quasars are fainter.

We thank Dr. R.E. Williams, Director of Cerro Tololo Inter-American Observatory for telescope time allocation. At Cerro Tololo O. Saá, D. Maturana and A. Gómez helped us with the plate acquisition. The ID charts were prepared by A. Fajardo at Cerro Calán. Computing facilities of the Centro de Procesamiento de Imágenes, Department of Astronomy, University of Chile, are gratefully acknowledged. This work was partially supported by FONDECYT (Fondo Nacional de Ciencias) grant # 89-992, and Departamento Técnico de Investigación, Universidad de Chile grant E2455-9055.

REFERENCES

Blanco, V.M. 1974, PASP, 86, 841
Gratton, R.G., & Osmer, P.S. 1987, PASP, 99, 899
Hoffleit, D. 1991, Vistas Astr., 34, 107
Høg E., von der Heide J., von Fischer-Treuenfeld F., Holst G., Loibl B., Zeigler U., Nikiloff I., & Helmer L. 1976, A Catalogue of Position of 24900 Stars, Hamburger Sternwarte
MacAlpine, G.M., & Lewis, D.W. 1978, ApJS, 36, 587
MacAlpine, G.M., & Williams, G.A. 1981, ApJS, 45, 113
MacAlpine, G.M., Lewis, D.W., & Smith, S.B. 1977, ApJS, 35, 203
MacAlpine, G.M., Smith, S.B., & Lewis, D.W. 1977*a*, ApJS, 34, 95
_____. 1977*b*, ApJS, 35, 197
Maza, J., & Ruiz, M.T. 1989, ApJS, 69, 353
_____. 1993, in preparation
Maza, J., & Takamiya, M. 1993, in preparation
Maza, J., Ruiz, M.T., González, L.E., & Wischnjewsky, M. 1988*a*, in Progress and Opportunities in Southern Hemisphere Optical Astronomy, eds. V.M. Blanco & M.M. Phillips, A.S.P.Conf.Ser. N°1, 410
_____. 1988*b*, in Proceedings of a Workshop on Optical Surveys for Quasars, eds. P.S. Osmer, A.C. Porter, R.F. Green, & C.B. Foltz, A.S.P.Conf.Ser. N°2, 154
_____. 1989, ApJS, 69, 349
_____. 1992, RevMexAA, 24, 147
Maza, J., Ruiz, M.T., M. Peña, González, L.E., & Wischnjewsky, M. 1991, A&AS, 89, 389
Maza, J., Ruiz, M.T., Wischnjewsky, M., González, L.E., & Antezana, R. 1993, in preparation
Pesch, P. 1991, in Objective-Prism and other Surveys, eds A.G.D. Philip & A.R. Upgren, (Schenectady, N.Y: Davis Press) 3
Schmidt, M. 1963, Nature, 197, 1040
Smith M.G. 1975, ApJ, 202, 591
Smith M.G., Aguirre C., & Zemelman M. 1976, ApJS, 32, 217
Stobie, R.S., Sagar, R., & Gilmore, G. 1985, A&AS, 60, 503
Weedman, D.W. 1986, in Quasar Astronomy, (Cambridge:Cambridge University Press), 64

Roberto Antezana, Luis E. González, José Maza, María Teresa Ruiz, and Marina Wischnjewsky: Departamento de Astronomía, Universidad de Chile, Casilla 36-D, Santiago, Chile.

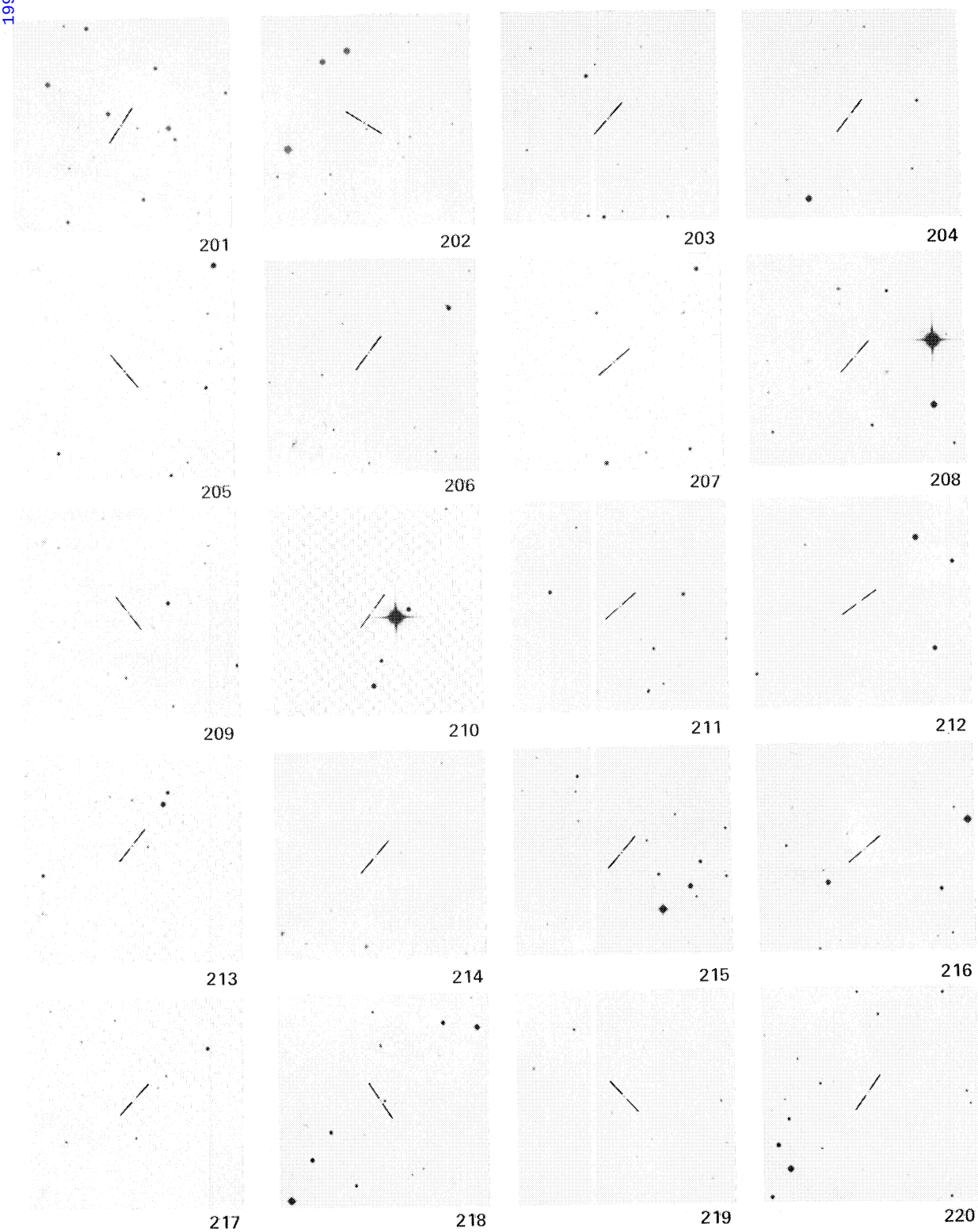

g. 1*a*. Objects 201-220. Finding charts for Calán-Tololo quasars from the ESO Quick Blue charts. North is to the top d east to the left. Each chart covers $9' \times 9'$.

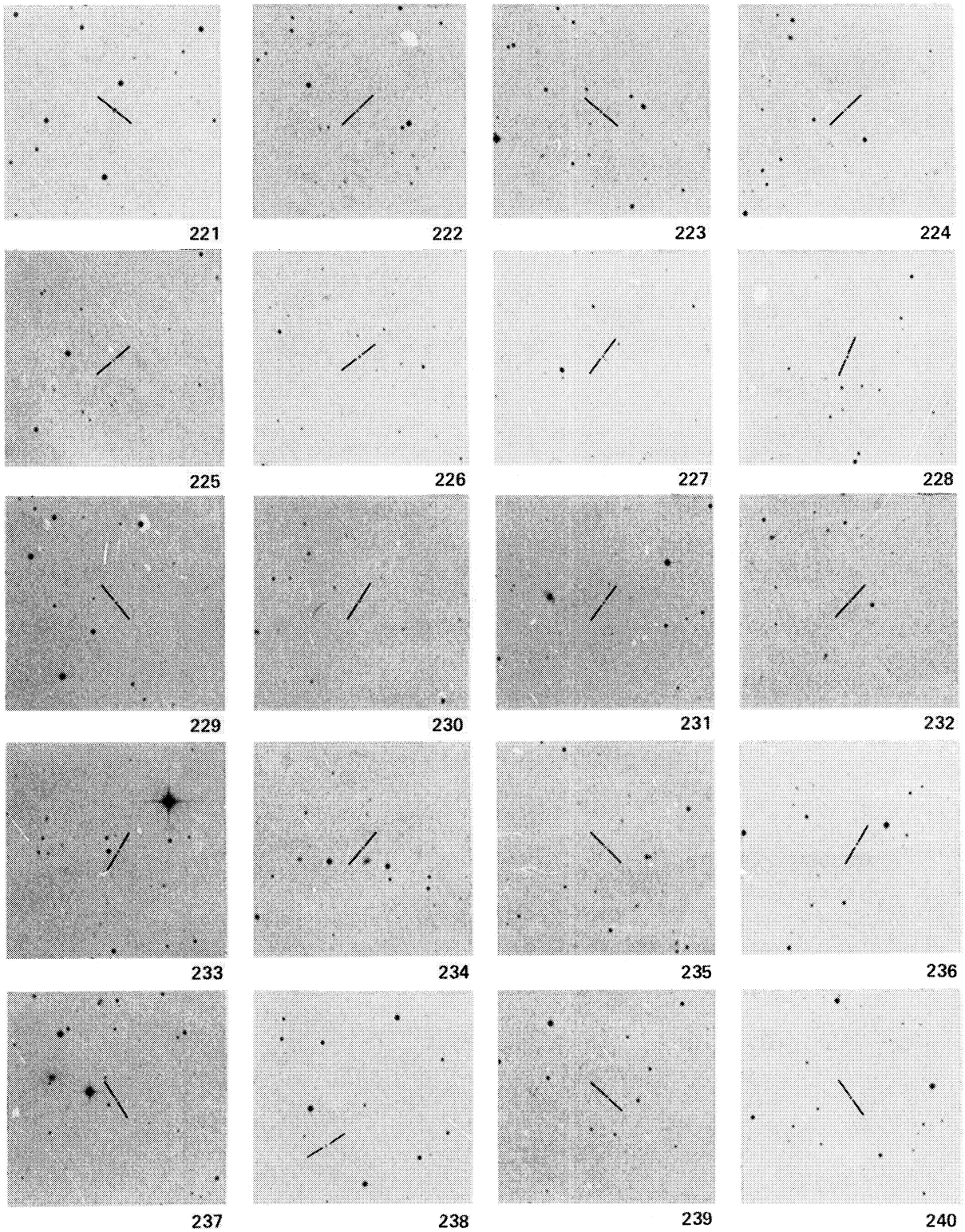

Fig. 1*b*. Same as Figure 1*a* for objects 221-240.

MAZA ET AL. (See page 51)

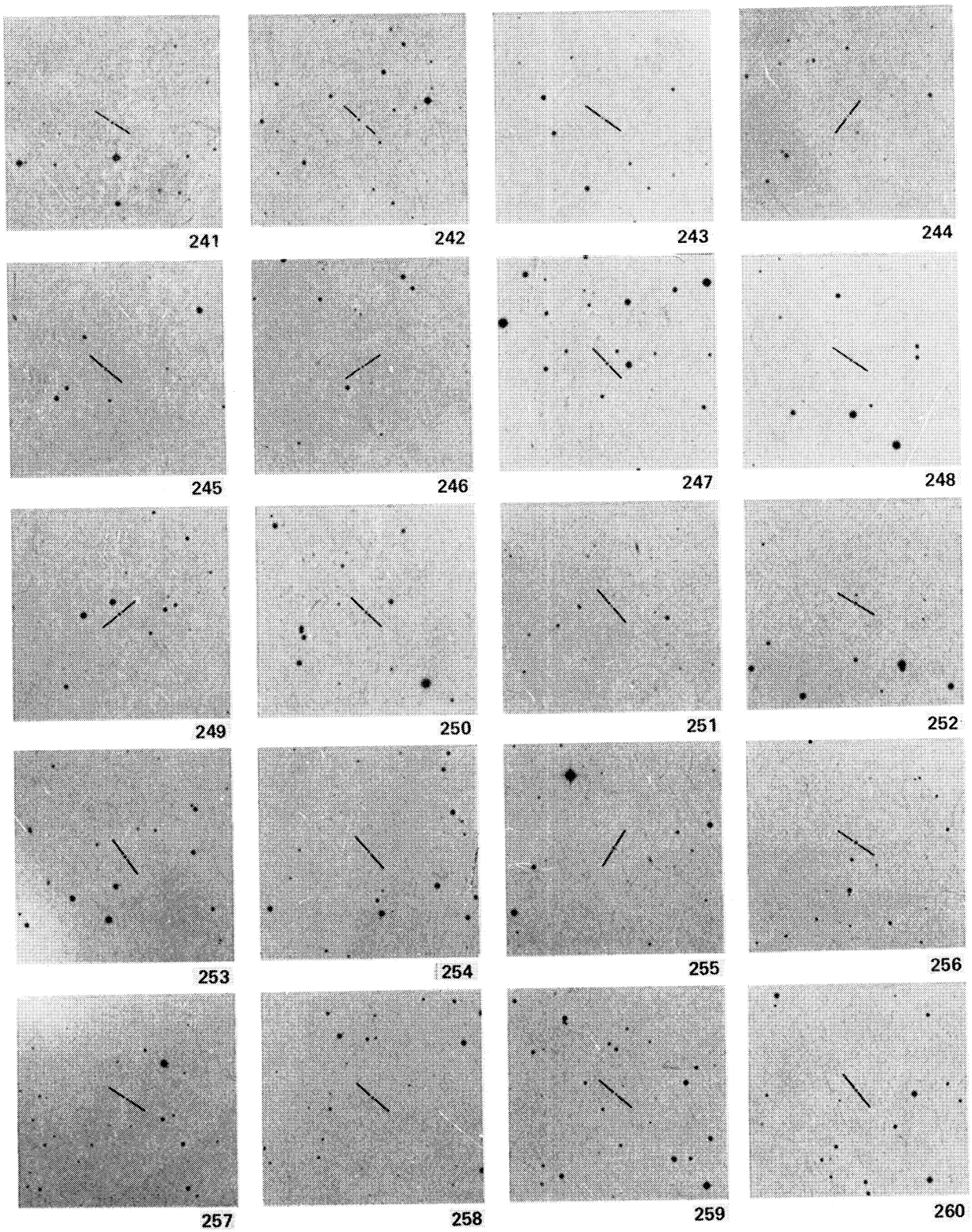

Fig. 1*c*. Same as Figure 1*a* for objects 241-260.

MAZA ET AL. (See page 51)

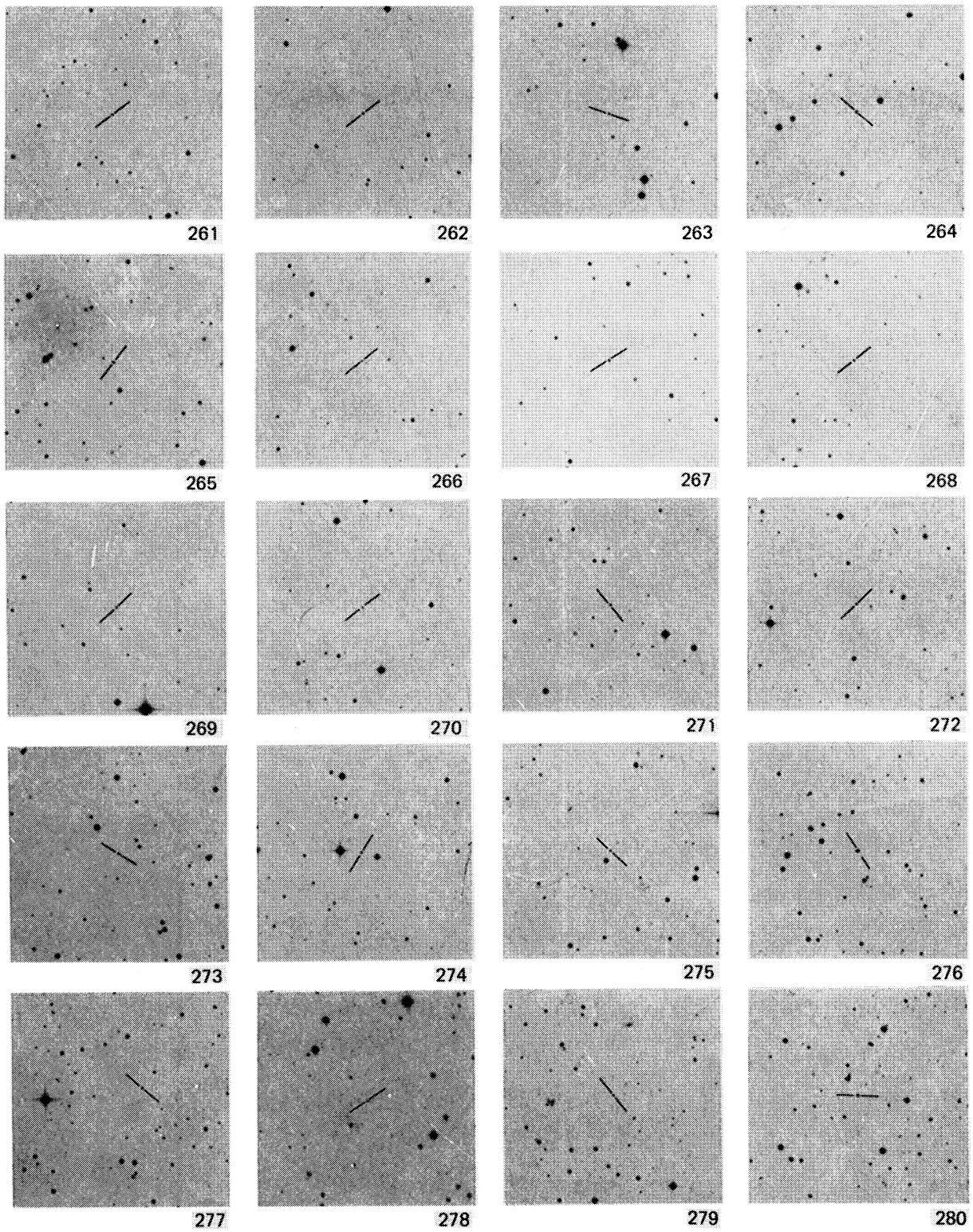

Fig. 1*d*. Objects 261-280. Finding charts for Calán-Tololo quasars from the ESO Quick Blue charts, except for object 278 for which a Maksutov plate was used. North is to the top and east to the left. Each chart covers $9' \times 9'$.

MAZA ET AL. (See page 51)

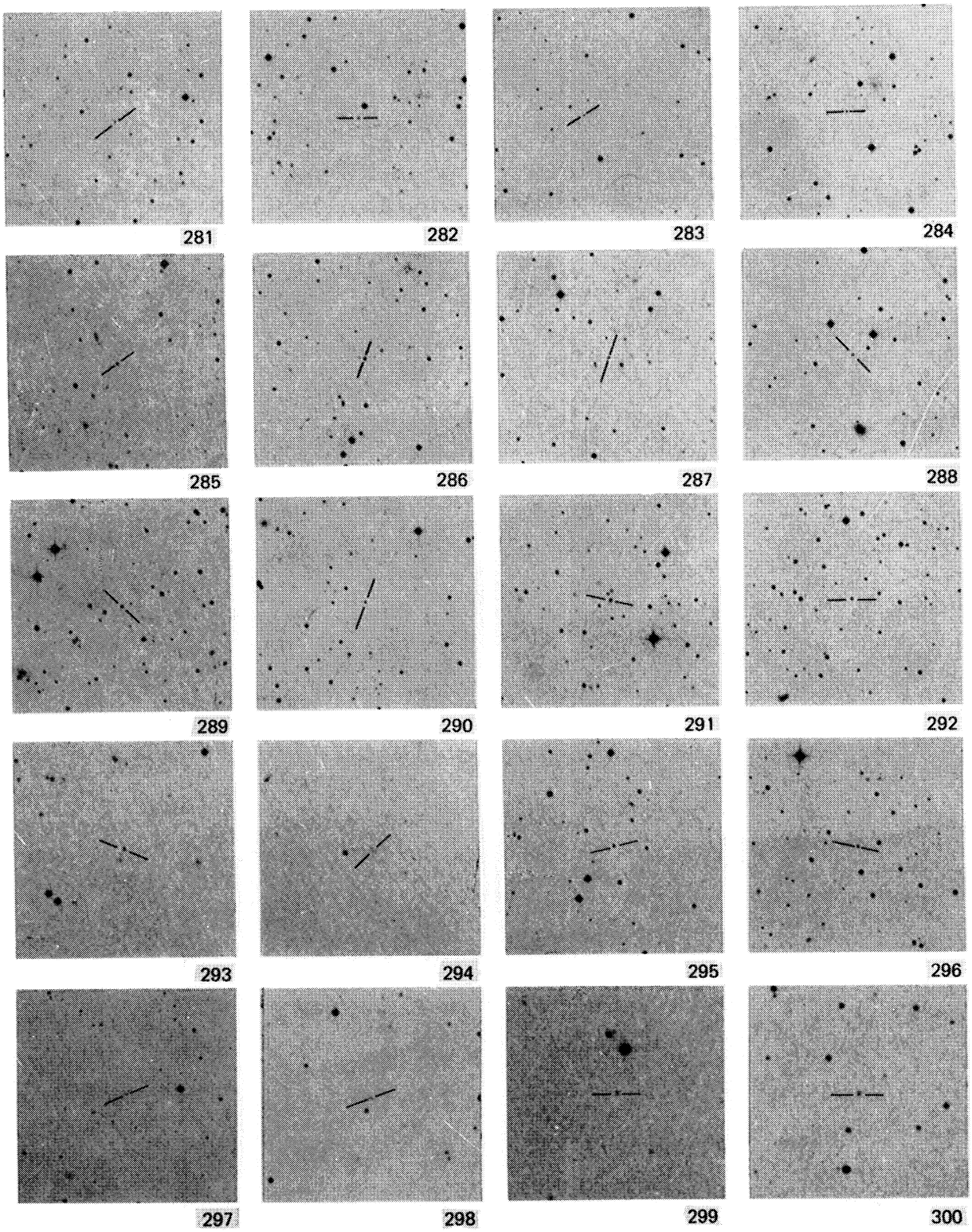

Fig. 1*e*. Objects 281-300. Finding charts for Calán-Tololo quasars from the ESO Quick Blue charts except for objects 285, 293, 294, 298, and 300, for which Maksutov plates were used. North is to the top and east to the left. Each chart covers $9' \times 9'$.

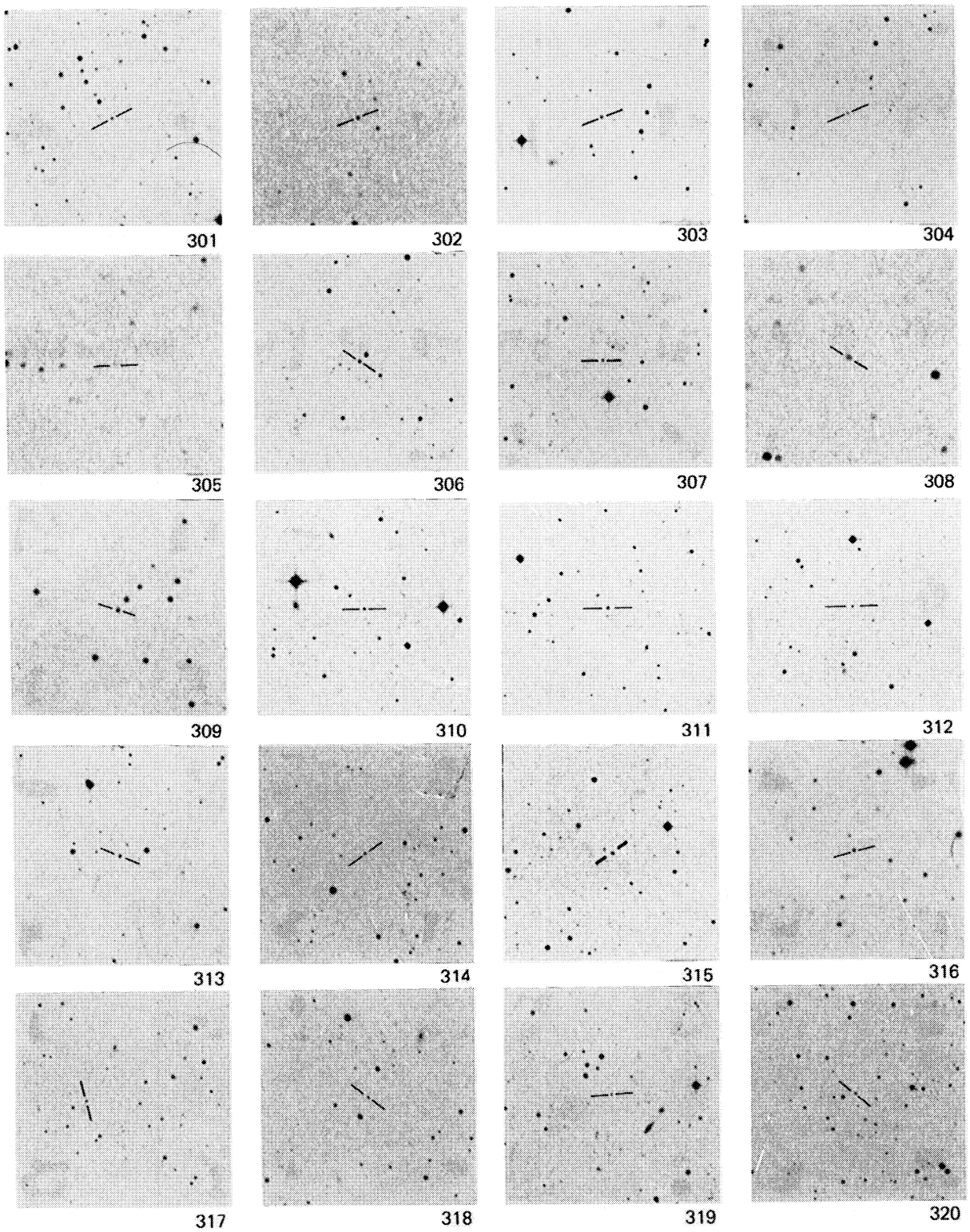

Fig. 1*f*. Objects 301-320. Finding charts for Calán-Tololo quasars from the ESO Quick Blue charts except for objects 302, 305, 308, 309, 310, 311, 312, 315, and 316 for which Maksutov plates were used. North is to the top and east to the left. Each chart covers $9' \times 9'$.

MAZA ET AL. (See page 51)

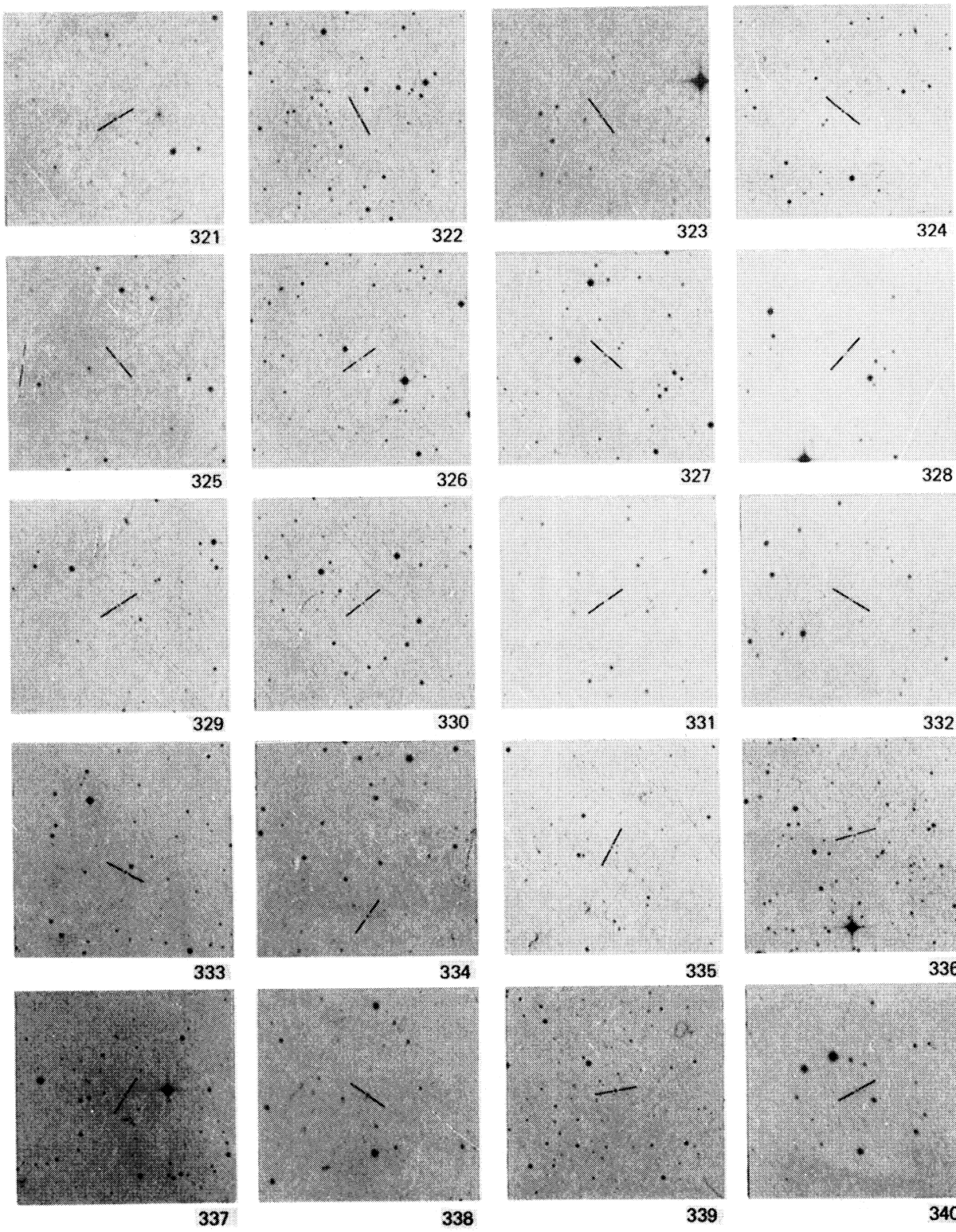

Fig. 1g. Objects 321-340. Finding charts for Calán-Tololo quasars from the ESO Quick Blue charts except for objects 321, 323, 325, 328, 331, 332, 334, 338, and 340 for which Maksutov plates were used. North is to the top and east to the left. Each chart covers $9' \times 9'$.

MAZA ET AL. (See page 51)

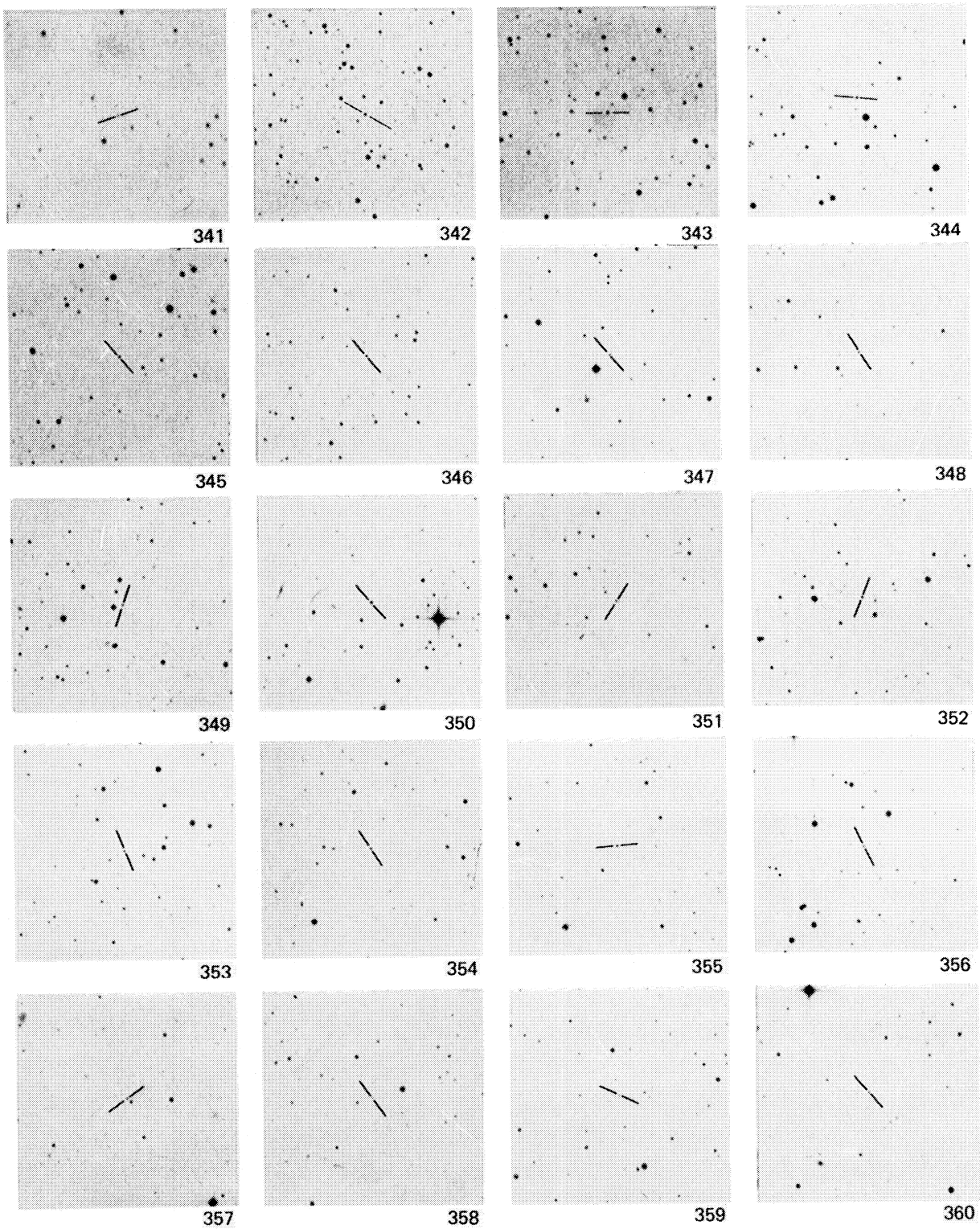

Fig. 1*h*. Objects 341-360. Finding charts for Calán-Tololo quasars from the ESO Quick Blue charts, except for object 341 for which a Maksutov plate was used. North is to the top and east to the left. Each chart covers $9' \times 9'$.

MAZA ET AL. (See page 51)

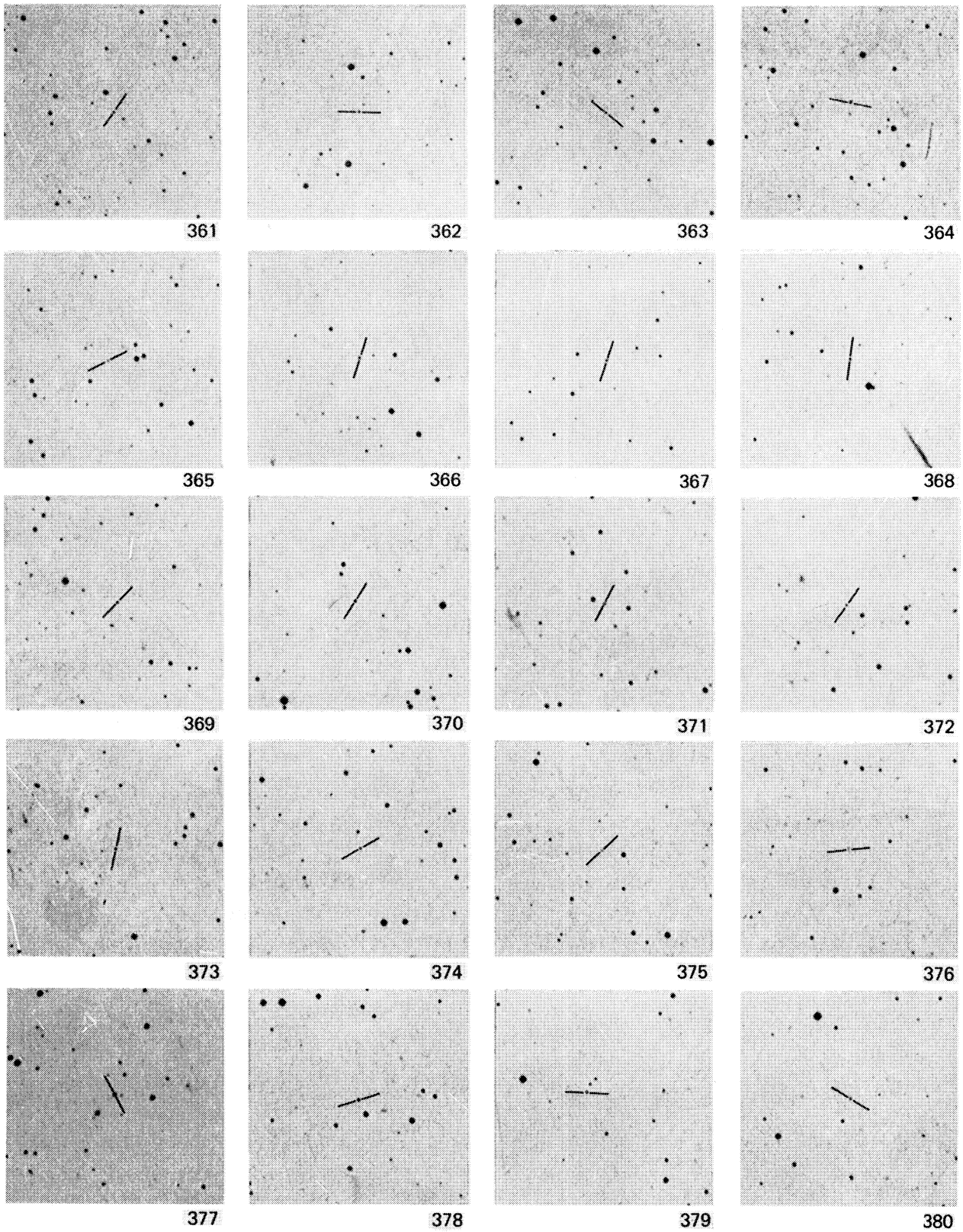

Fig. 1*i*. Same as Figure 1*a* for objects 361-380.

MAZA ET AL. (See page 51)

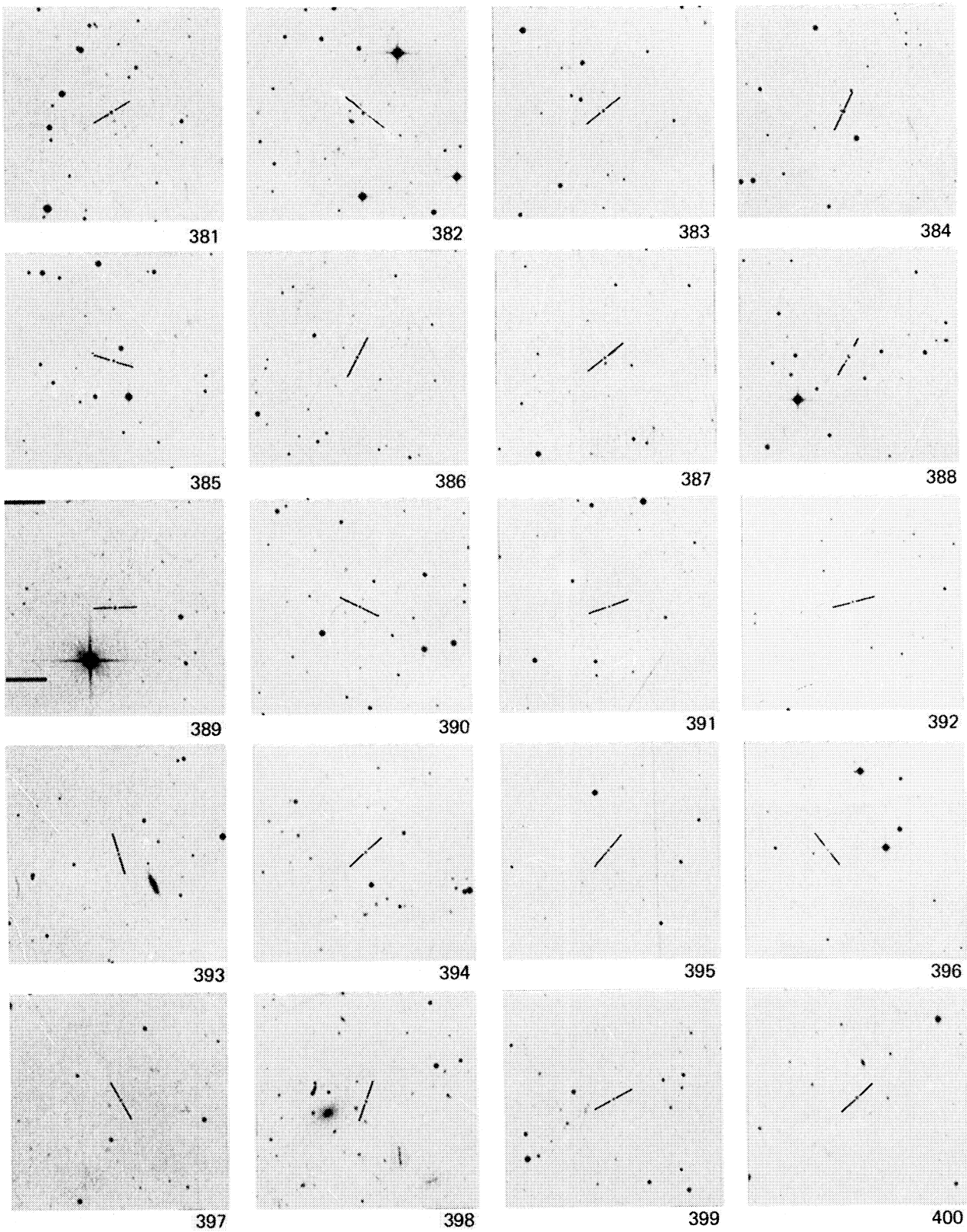

Fig. 1*j*. Same as Figure 1*a* for objects 381-400.

MAZA ET AL. (See page 51)